ROCK PHYSICS CONSIDERATION OF DYNAMIC FRICTION IN METHANE HYDRATE BEARNG SEDIMENTS AS ONE OF MECHANISMS OF S-WAVE ATTENUATION

（メタンハイドレート堆積物における S 波減衰機構の一つとしての
動摩擦に関する岩石物理学的検討）

47216779 NIU Zihan
Expected graduation: September 2023
Supervisor: Prof. Jun Matsushima

Abstract: The exploration of Methane Hydrate (MH) is quite essential for its holding great potential as an alternative energy source and possesses significant implications for global climate change and sub-marine geohazards. Recent S-wave attenuation estimation in methane hydrate bearing sediments shows low frequency dependence between sonic logging and seismic exploration frequencies. However, existing rock physics models cannot explain such frequency independence and further underestimate the magnitude of S-wave attenuation. This study formulates a rock physics model that integrates dynamic friction on the contact lines as a contributing mechanism for S-wave attenuation. The simulation results show that the friction occurring at the three-phase contact line between methane hydrate, sand grains, and seawater engenders considerable dissipation. Also, the shear wave attenuation predicted by this model fits well with the attenuation estimated from walkaway vertical seismic profiling (w-VSP) exploration data, and exhibits low frequency dependency. We draw the conclusion that the dynamic friction on the contact line might be the main mechanism of shear wave attenuation.

Keywords: methane hydrate bearing sediments, S-wave attenuation, rock physics modeling, frequency dependence, contact line

Introduction

Methane Hydrate (MH) holds great potential as an alternative energy source and possesses significant implications for global climate change and sub-marine geohazards. Geophysical exploration plays a crucial role in the identification and characterization of sediment formations containing methane hydrate (MH), including parameters such as hydrate saturation, lithology, permeability, porosity, and the extent and thickness of MH-bearing sediments. Among the various geophysical techniques, seismic methods are widely used for MH detection. Rock physics modeling allows the estimation of seismic velocity based on seismic data, which can be correlated with hydrate saturation.

In this research, sonic and VSP (Vertical Seismic Profiling) data were collected in the Nankai Trough, which is situated beneath the Pacific Ocean off the southeastern coast of Japan. The sonic log waveform data and the attenuation values derived from the walkaway vertical seismic profiling (w-VSP) waveform data were compared and the S-wave attenuation found to have weak frequency-dependence.

There are some theories explaining the mechanisms of wave attenuation in MHBS. In terms of S-wave attenuation, the most widely approved theory is proposed by Guerin & Goldberg (2005), the base of which is Biot type three-phase theory (Biot, 1956) and was optimized by Leclaire et al. (1994) and Carcione & Tinivella (2000). Zhan (2020) averaged the sonic S-wave attenuation values calculated by Suzuki & Matsushima (2013) under each scale of MH saturation, and compared them with the predicted values by the models mentioned above. Among these predictions, the attenuation by the Leclaire model is significantly lower than those of the Carcione and Guerin models, and also than the averaged values even minus the standard deviation. As for the largest prediction case (under certain sand and hydrate permeability), the predicted values are overall 20 percentage points lower than the measured values.

In this work, we attempted to consider the dynamic friction on the contact line as the main mechanism of the S-wave attenuation. But so far, the mechanisms and the influence factor of the value of contact line friction have not been clear. To mathematically describing the reservoir and its petrophysical properties, we used the Representative Element Volume (REV) concept proposed

by Lie and Mallison (2015). Rozhko (2021) designed an REV-concepted model to simulate the P-wave case and found that the friction on the contact line is significantly underestimated. The author also conducted Fourier analysis to the strain data of the REV and observed new low frequency is generated (under bi-sinusoidal wave and Ricker wave), which appears as low-frequency shadows in seismic exploration, which is another sign of reservoir of hydrocarbon. We extended the research of Rozhko (2021) to consider the case of S-wave and calculated using the Muskhelishvili's Potentials and setting a stepping system to simulate the wave. Finally, we validated the model in two ways, the first is to compare the simulated attenuation data with the w-VSP data from the situ field, and the other is detect the low-frequency shadows. We predict the attenuation at broadband frequencies based on S-wave attenuation from w-VSP and sonic logging data. In order to emphasize that the viscosity dissipation has minimal impact on the attenuation, this time we regarded the methane hydrate as a kind of viscous liquid. And according to Ecker et al. (1998), the methane hydrates are mainly generating away off the connect of the grains, which cause the penetration of the MHBS to be very low, especially near the bottom simulation reflector, so there are few gases in the sediments. In this work, the three phases to form the contact are methane hydrate, sand grains and sea water.

Method

As for the method, we developed mathematical equations for the dynamic friction on the contact line to calculate S-wave attenuation. The constructing process, assumptions, input parameters, and workflows are stated as follows.

First, we used the same REV in Rozhko (2016). This model can consider three phase cases. In the static analysis part, we used Muskhelishvili's method (Muskhelishvili, 1977) to get the relationship between the far field stress plus the pressure of the enclosure liquid and the displacement of any point in the REV. Three cases, REV with empty, totally saturated and partially saturated crack were calculated, respectively. The first two cases were calculated to compare the results with previous research in order to validate methods. After that, we used geometric relationships in the partially saturated REV to construct the digital correlation between wave, sand and the drop. Finishing the static analysis part, cyclic stress was applied to the model, and the deformation of the REV was regarded as a quasistatic progress. From one step to next step, all the one-dimensional physical quantities were taking linear continuous changes, and once the far field stress stopped change at one step, the other quantities stopped change at the step as well.

In the dynamic analysis part, a stepping system was used to describe the behavior of the contact line, because the deformation of the liquid was not linear as a result of contact line hysteresis. This suggests that the quantities change on both sides of one step could be nonlinear. Like one quantity stays increasing before one step but after the step it begins to drop. This does not conflict with the linear change between steps stated in the previous paragraph. On each step, what we calculate includes the deformation of the liquid and the rock (sand), and the internal force of the REV. In this part we also conducted the calculation on the test cases. After the deformation of the REV in one cycle of the far field stress was simulated, we calculated the stored energy and dissipated energy, and finally estimated the quality factor from them.

In this work, an REV is defined as a piece of rock including a crack, shown in Fig. 1(a) The crack is approximated by an elliptical cavity with the major axes of length 2a and minor axes of length 2b. In the crack, a drop of liquid is contacting the top and bottom of the crack, and the length of the wetting part is 2c. The xy section is shown in Fig. 1(b). The rock was subject to uniform pressure P_{we} from the liquid drop on the boundary of the crack, and P_{nw} from the other parts of the boundary. In this model, the wetting part means connecting with (wetted by) methane hydrates, and the non-wetting parts were saturated by sea water. The applicability of this model is considerable because if we consider the fourth phase – gas, we can still use this REV, by just adjusting the proportion of the pore number. Anyway, in this work we do not consider gas – according to Ecker et al. (1998), the methane hydrates are mostly generated away off the connects of the sand grains, so they block the pores, which cause the permeability of MHBS to be very low. This also explains why there are plenty of suspended gas under the BSR. On the other hand, there is no significant reflector above the methane region, this means that the saturation of methane hydrate reduces as the depth decreases, which denotes that the small amount of gas escaping from under the BSR can easily get up to the sea. So, the gas saturation in the MHBS can be very low.

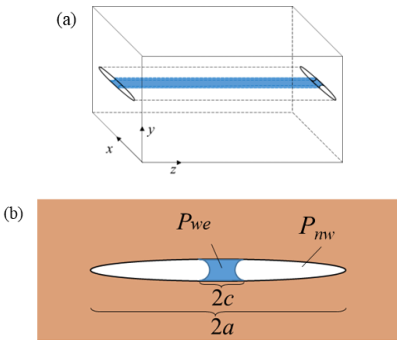

Fig. 1. (a) Representative volume element containing a partially saturated crack, approximated by an elliptical cavity of high aspect ratio, where 2a is major axis of ellipse. (b) The horizontal section of the model. Plane-strain approximation is used, which implies that a variation of geometry, far-field stresses and fluid pressure in z-direction is neglected. Partially saturated crack with the wetting fluid phase located symmetrically at the tips, under pressure P_{we}. The non-wetting fluid phase is located at the center, under pressure P_{nw}. The length of the interface meniscus is 2c.

In the static analysis part, only static far-field stress acts on the body. The strain of every point in the body was calculated according to Muskhelishvili (1977), in which the author offered a method with a pair of

Kolosov-Muskhelishvili potentials that can express all the parameters including stress and strain of the points in the body. There is no actual physical quantity corresponding to these two potentials. We can understand them as potential functions and stream functions in fluid mechanics. In this part, we can get the displacement of every point in the REV under arbitrary certain stress condition.

In the dynamic analysis part, when the shear wave propagates through the REV, the crack begins to deform, and the liquid drop will follow so, which will cause the contact angle to get larger on one side and smaller on the other side (shown in Fig. 2). It is because there is dynamic friction on the contact lines that they do not move once there is deformation. Then we started the stepping simulation. The initial value of *m* was 0. Every step we calculate the variation of *n*, *dn* and made a judgement: if this step's *m* plus *dn* exceeds the range [-m_0,m_0], *m* stays the original value; if not, *m* returns *m*+*dn*. And the relative velocity of the two layers can also be calculated by *dn*/step size (for the definition of m and n, see Fig. 2). After the one period of simulation, we calculate the attenuation factor.

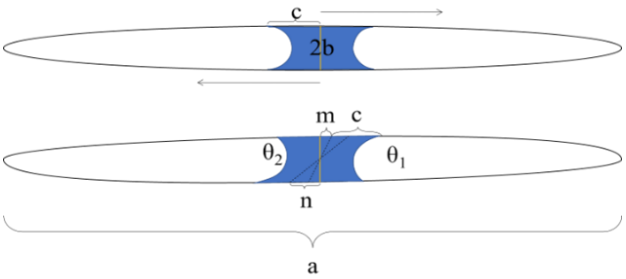

Fig. 2. The draft of deformation of the crack and the liquid drop. The *m* is the displacement of the midpoint of the liquid drop, the *n* is that of the crack, and *c* is the half width of the hydrate drop.

Fig. 3. The displacement of the hydrate drop midpoint.

In Rozhko (2021), P-wave is applied to the REV and low-frequency shadows are detected under bi-sinusoidal waveform and Licker waveform. In this work, the same operation is applied to the shear bi-sinusoidal case. After we finished the dynamic analysis, we let the stress wave continue to act for tens of cycles, get the data of the midpoint displacement of the crack boundary under multiple cycles, and carried out Fourier analysis on it.

Input parameters

The properties of the hydrate, sand and sea water referred to the coring data of situ samples, laboratory artificial samples and their physical and chemical properties. The exact value of the parameters in the model are listed in Table 1.

Results

Fig. 4(a) shows the S-wave attenuation predicted by our contact line friction model. The saturation range starts from 10% because when it is 0 there will be errors in the calculation of m0. The results indicate that the attenuation is strongly dependent on the range of contact angle (Case 1 and Case 2), because this range determines the duration of work done by contact line friction. Under the contact line ranging from 25°~30°, the attenuation predicted fits well with the measured data. Under different frequency of the wave (Case 1 and Case 3), the attenuation has low difference, which also matches the low difference between the actual data from w-VSP and sonic attenuation. The S-wave attenuation is predicted better than that of using optimized Leclaire, Carcione, and Guerin models calculated by Zhan (2020).

Fig. 4(b) shows the Fourier spectrum of crack boundary displacement and the stress of the wave. No new low frequency is generated in the displacement data like the situation in Rozhko (2021). This result also conforms to the situ results in S-wave case. In this aspect the contact line friction model is proved reasonable.

By construct a model considering the dynamic friction on the contact line and compare the prediction with the w-VSP data in situ area, we infer that the friction between hydrate and sand grains is a reasonable mechanism of the S-wave attenuation. And we also draw the conclusion that the dynamic friction dominates the S-wave attenuation much more than viscous friction for the small difference between different frequencies. Finally, the effect of dynamic friction which is not frequency-dependent may explain the weak frequency-dependence of S-wave attenuation between sonic logging and seismic frequencies.

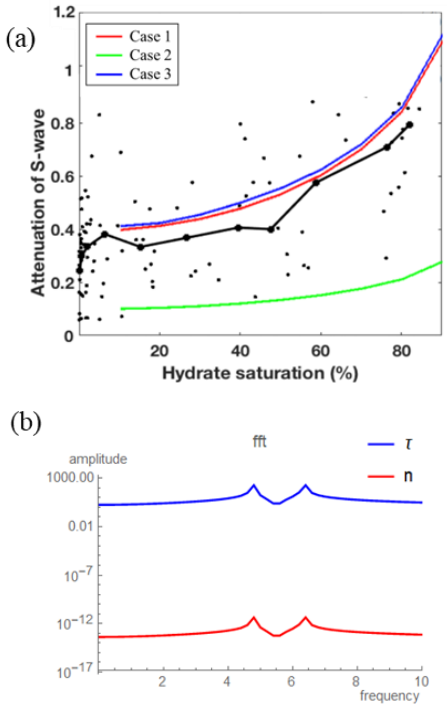

Fig. 4. (a) Measured S-wave attenuation (black lines) and predicted attenuation by contact line friction model (colored lines) of difference cases: Case 1 (wave frequency – 40 rad/s, contact angle – 25°~30°), Case 2 (wave frequency – 40 rad/s, contact angle – 20°~60°) and Case 3 (wave frequency – 400 rad/s, contact angle – 25°~30°). (b) Fourier spectrum of the crack boundary displacement (*n*) and the stress of the wave (τ).

Table 1. Input parameters in the concact line friction model.

	Case 1	Case 2	Case 3
Young's modulus (E) (MPa)	300	300	300
Poisson's ratio (v)	0.3	0.3	0.3
Surface tension (γ) (Pa · m)	0.072	0.072	0.072
Advancing contact angle (θ_a) (°)	30	60	30
Receding contact angle (θ_r) (°)	25	20	25
Effective stress (τ) (MPa)	10	10	10
Major semiaxis (a) (m)	3×10^{-7}	3×10^{-7}	3×10^{-7}
Minor semiaxis (b) (m)	2×10^{-7}	2×10^{-7}	2×10^{-7}
Porosity (n_{cr}) (%)	43	43	43
Viscosity of water (η_w) (Pa·s)	1.1×10^{-3}	1.1×10^{-3}	1.1×10^{-3}
Viscosity of methane hydrate(η_m) (Pa·s)	0.5	0.5	0.5
Frequency of sinusoidal wave (rad/s)	40	40	400

Discussion and Conclusions

The present study demonstrated the significant S-wave attenuation at seismic frequencies from w-VSP data acquired in the MHBS, which implies weak frequency-dependence of S-wave attenuation in MH reservoirs. By construct a model considering the dynamic friction on the contact line and compare the prediction with the w-VSP data in situ area, we infer that the friction between hydrate and sand grains is a reasonable mechanism of the S-wave attenuation. And we also draw the conclusion that the dynamic friction dominates the S-wave attenuation much more than viscous friction for the small difference between different frequencies. Finally, the effect of dynamic friction which is not frequency-dependent may explain the weak frequency-dependence of S-wave attenuation between sonic logging and seismic frequencies.

Theoretically, the attenuation by the contact line friction model under 0 hydrate saturation should be around 0 (only viscous dissipation), which conflicts with the measured data. We speculate that there are some gas bubbles in the low hydrate saturation areas, because in these areas, the permeability of the sediments is much higher than high saturation areas. By simulation, the contact line friction between the three phases of water, gas and sand also causes considerable energy dissipation. This might be the reason why there is still attenuation around 0.3 in the 0 hydrate areas.

The contact line friction model regards the methane hydrate as a kind of viscous liquid. For the exact property of it under the condition of deep seabed, we still need more laboratory data support. Another conjecture is that methane hydrate exhibits solid properties when it rubs against rocks, which can also be verified through simulation experiments. Both the ideas base on the AVO analysis done by Ecker et al. stating that there is no cementing morphology in the MHBS.

Reference

[1] Guerin, G., & Goldberg, D. (2005). Modeling of acoustic wave dissipation in gas hydrate-bearing sediments. Geochemistry, Geophysics, Geosystems, 6, Q07010.

[2] Biot, M. A. (1956a). Theory of Propagation of Elastic Waves in a Fluid-Saturated Porous Solid. I. Low-Frequency Range. The Journal of the Acoustical Society of America, 28(2), 168–178. https://doi.org/10.1121/1.1908239

[3] Leclaire, P., Cohen-Ténoudji, F., & Aguirre-Puente, J. (1994). Extension of Biot's theory of wave propagation to frozen porous media. The Journal of the Acoustical Society of America, 96(6), 3753–3768. doi:10.1121/1.411336

[4] Carcione, J. M., & Tinivella, U. (2000). Bottom-simulating reflectors: Seismic velocities and AVO effects. Geophysics, 65(1), 54–67. Retrieved from

[5] Zhan, L. (2020). ROCK PHYSICS STUDY ON THE FREQUENCY DEPENDENCE OF SEISMIC ATTENUATION IN METHANE HYDRATE-BEARING SEDIMENTS. Doctoral Thesis.

[6] Suzuki, H., & Matsushima, J. (2013). Quantifying uncertainties in attenuation estimation at methane-hydrate-bearing zones using sonic waveform logs. Geophysics, 78(5), D339–D353. doi:10.1190/GEO2012-0495.1

[7] Lie, K.-A. and Mallison, B.T. (2015). Mathematical Models for Oil Reservoir Simulation. pp.850–856.

[8] Rozhko, A.Y. (2021). On the spectral changes of seismic wave energy by a partially saturated crack due to the hysteresis of liquid bridges phenomenon. 86(3), pp.MR133–MR147. doi:https://doi.org/10.1190/geo2020-0685.1.

[9] Ecker, C., Dvorkin, J., & Nur, A. (1998). Sediments with gas hydrates: Internal structure from seismic AVO. Geophysics, 63(5), 1659. doi:10.1190/1.1444462

[10] Rozhko, A.Y. (2016). Two-phase fluid-flow modeling in a dilatant crack-like pathway. Journal of Petroleum Science and Engineering, [online] 146, pp.1158–1172.

[11] N.I. Muskhelishvili, Some Basic Problems in the Mathematical Theory of the Elasticity, Springer, Berlin (1977)

[12] Johansson, P. & Hess, B. (2018). Molecular origin of contact line friction in dynamic wetting. Physical Review Fluids, 3(7).

[13] Adam, N.K. & Jessop, G. (1925). CCL.—Angles of contact and polarity of solid surfaces. J. Chem. Soc., Trans., 127(0), pp.1863–1868.